Hyperfine Interact (2017) 238:2
DOI 10.1007/s10751-016-1373-7

In and Cd as defect traps in titanium dioxide

Juliana Schell[1,2] · Doru C. Lupascu[2] · João Guilherme Martins Correia[1,3] · Artur Wilson Carbonari[4] · Manfred Deicher[5] · Marcelo Baptista Barbosa[6] · Ronaldo Domingues Mansano[7] · Karl Johnston[1] · Ibere S. Ribeiro Jr.[4] · ISOLDE collaboration[1]

Abstract We present a study of TiO_2 single crystals from the point of view of the dopant atom that simultaneously behaves as the probing element. We used gamma-gamma time dependent perturbed angular correlations working with selected tracer elements (^{111}In/^{111}Cd, ^{111m}Cd/^{111}Cd) together to investigate the different behavior of Cd and In dopants, particularly their interaction with point defects in the TiO_2 lattice. Results show that the hyperfine interactions observed at ^{111}Cd from ^{111}In or ^{111m}Cd decay are quite different. ^{111}In/^{111}Cd results show a single site fraction characterized by a quadrupole frequency with asymmetry parameter similar to those observed for the same probe nuclei in bulk TiO_2 oxides. Results for ^{111m}Cd/^{111}Cd reveal two site fractions, one characterized by the same hyperfine parameters to those measured in bulk TiO_2 and another fraction characterized by a quadrupole frequency and asymmetry parameters with higher values, as observed in thin

This article is part of the Topical Collection on *Proceedings of the International Conference on Hyperfine Interactions and their Applications (HYPERFINE 2016), Leuven, Belgium, 3-8 July 2016*
Edited by Kristiaan Temst, Stefaan Cottenier, Lino M. C. Pereira and André Vantomme

✉ Juliana Schell
juliana.schell@cern.ch

[1] European Organization for Nuclear Research (CERN), CH-1211 Geneva, Switzerland

[2] Institute for Materials Science and Center for Nanointegration, Duisburg-Essen (CENIDE), University of Duisburg-Essen, 45141 Essen, Germany

[3] C^{2}TN, Centro de Ciências e Tecnologias Nucleares, Instituto Superior Técnico, Universidade de Lisboa, Lisbon, Portugal

[4] Instituto de Pesquisas Energéticas e Nucleares, Universidade de São Paulo, São Paulo, Brazil

[5] Experimentalphysik, Universität des Saarlandes, Saarlandes, Germany

[6] Instituto de Física dos Materiais da Universidade do Porto, Porto, Portugal

[7] Escola Politécnica, Universidade de São Paulo, São Paulo, Brazil

Published online: 30 November 2016

TiO_2 films and correlated with point defects. The results are discussed emphasizing the differences for Cd and In as defect traps on TiO_2.

Keywords In and Cd doping · Gamma-gamma PAC · Titanium dioxide

1 Introduction

Pure or doped TiO_2 have diversified applications such as photo-catalyst for water and air purification, energy converter in solar cells and sunscreen material for UV light protection, which are just a few uses that reveal its rich set of electronic and chemical properties making it further attractive to the electronics industry [1–3]. The particular case of Cd-doped TiO_2 shows higher diffuse reflection under visible light with lower resistance and smaller band gap than undoped TiO_2 [4]. There exist different polymorphs of TiO_2, where the main crystalline structures are anatase (space group $I4_1/amd$) and rutile (space group $P4_2/mnm$), both with tetragonal structure. On doped TiO_2 we particularly stress that the lattice position of the dopant rules both electronic properties and thermodynamic stability [5].

In what concerns the panorama of *local probe* doping studies on TiO_2, we point the former work of Adams and Catchen [6] studying the temperature dependence of hyperfine parameters of rutile TiO_2 in the temperature range from 290 to 1300 K using ^{111}In/Cd and ^{181}Hf/Ta as PAC probe nuclides. The ^{111}In/Cd PAC experiments shown that the axial asymmetry parameter, η, of the Electric Field Gradient, EFG, decreases with raising temperature up to 700 K. In the temperature range from 700 to 800 K η essentially vanishes and it increases above 800 K (these results are in qualitative agreement with NMR measurements); the authors observed a monotonically decrease of the principal EFG component, V_{zz}, as the temperature increases. When using ^{181}Hf as a probe nucleus almost no variation of η with a slight increase of V_{zz} were observed upon raising temperature, as observed in implanted thin films by Schell [7]. The authors justified the different results observed for ^{111}In/Cd and ^{181}Hf/Ta in rutile TiO_2 as a result of the different electronic structures and ionic size of the probe nuclides. Darriba et al. [8], performed new PAC measurements with ^{181}Hf/Ta in the range from 273 to 1273 K in rutile TiO_2 single crystal and discussed the results with the help of hyperfine parameters obtained by first-principles calculations. The experimental values of η and V_{zz} obtained in this work as a function of the temperature are in agreement with those achieved by Adams and Catchen [6]. Darriba et al. confirmed that the charge state of the ^{181}Hf impurity induces no significant differences in the EFG tensor, whereas the expected EFG dependence on the charge state of Cd are remarkable. Darriba et al. explain such behavior by different local relaxations that the impurities induce in TiO_2. It happens because a metallic system is formed when a Cd atom replaces a Ti atom in the super cell due to the two electrons that are necessary to fill the O p band, and therefore occurs a change in the symmetry of the electronic charge in the impurity neighborhood. The little variation of V_{zz} and η with temperature, in the case of ^{181}Hf replacing the Ti atom in TiO_2, was explained by using first principles calculations, introducing a thermal expansion coefficient of the TiO_2 lattice, in agreement with the experimental results. More recently, using the fact that ^{181}Hf/Ta are quite stable elements on TiO_2, Banerjee et al. [9] have probed structural phase transitions in nanostructured samples. On the other hand, we might expect a more important and distinguishable role and on defect trapping for Cd and In atoms dopants in the TiO_2 lattice.

Defects produced during implantation of dopants result from knock-out changes of atomic positions merged together with an increasing concentration of point defects within a small space region. Moreover, there is additional interest in comparing experiments performed with different implanted dopants, since they do not necessarily go to the same lattice sites, nor have the same charge states, with clear consequences on the doping effect. Since local distortions and defect trapping lead to radical changes of the electric field gradients at the probe dopant lattice site, which can then be measured with the PAC technique and, in this way, identified. Consequently, the evolution of defect recovery and/or of phase transitions can be studied as a function of annealing and/or measuring temperature with high resolution at the atomic scale with a sensitivity far above the capabilities of traditional diffraction or macroscopic techniques. In the particular case of In and Cd when replacing titanium, which has a +4 valence, both elements need to achieve charge balance. Furthermore, Cd needs an additional load regarding In that can then contribute to the formation or trapping of defects such as oxygen vacancies.

In this work we have studied ^{111}In/Cd and ^{111m}Cd/Cd also simultaneously and dopant incorporation on TiO_2 by ion implantation with the perturbed gamma-gamma angular correlation (PAC) technique. These experiments were carried out at the on-line isotope mass separator ISOLDE/CERN. So far there was no previous work reporting comparative studies of ^{111}In/Cd and ^{111m}Cd/Cd implanted together.

2 Perturbed angular correlations

Using Perturbed Angular Correlations [10, 11] it is possible to measure electric field gradients and magnetic fields by hyperfine interaction with radioactive probe nuclei with very small concentrations of the implanted probe (typically 10^{12} probe nuclei). Due to these small concentrations, the underlying structure of the system under investigation is essentially unaltered and an unambiguous picture of physical processes can be obtained, in some cases after annealing to recover the implantation damage. When the probe atom is located on the substitutional site, the detrimental effects of ion implantation are minimal and thus not disturbing the study of the component of interest. Therefore, this class of materials is very well suited for the PAC measurements. The PAC measures the perturbation function R(t) for different cases, as shown in the (1):

$$R\,(t) \approx A_{22}G_{22}\,(t) \tag{1}$$

The perturbation factor is given by the (2) for one "sharp" EFG in polycrystalline samples.

$$G_{22}\,(t) = s_{20} + \sum_{n=1}^{3} s_{2n}\cos\,(n\omega_0 t) \tag{2}$$

For the case of single crystalline samples the coefficients s_{2n} depend on the orientation of the main axis of the EFG tensor relative to the emission directions of the γ-rays.

The asymmetry parameter $\eta = (V_{xx} - V_{yy})/V_{zz}$, describing the asymmetry of the EFG tensor, is obtained from the ratio ω_2 / ω_1 which varies between 2 and 1 for $0 \leq \eta \leq 1$.

If there are probe atoms exposed to $j$different microscopic environments, each of them

creating a characteristic field gradient at the fraction f of probe atom sites, the perturbation function becomes:

$$\mathrm{G\,(t)} = \sum_{\mathrm{j}} f_{\mathrm{j}} \mathrm{G_j\,(t)} \tag{3}$$

Experiments require the introduction of a radioactive probe into a material – most typically via implantation, but diffusion and other methods are also possible. Once the radioactive probe is inside the host material, local information is obtainable on a nanosecond/microsecond timescale. PAC spectroscopy provides information via hyperfine interactions between the extra-nuclear electromagnetic fields (electric field gradient, *EFG*, and magnetic hyperfine field, B_{hf}) and the nuclear magnetic dipole and/or the electric quadrupole moment of the radioactive probe nuclei embedded in the material to study.

PAC measurements can be performed as a function of annealing and measuring temperature to study the defect recovery after the implantation of potential dopants. In practice, the B_{hf} can be obtained from the observable Larmor frequency, ω_L, and the major component of the EFG tensor V_{zz} can be obtained by the observable spin dependent quadrupole frequency $\omega_Q$expressed, respectively, as:

$$\omega_L = -g\frac{\mu_N}{\hbar}B_{hf} \quad ; \quad \omega_Q = \frac{eQV_{zz}}{4I\,(2I-1)\hbar}, \tag{4}$$

with g (gyromagnetic factor), μ_N (nuclear magneton), I (nuclear spin) and Q (nuclear quadrupole moment). In this paper we focus on electric hyperfine interactions, since there is no evidence of ferromagnetism involved in our studies. Nuclear quadrupole interaction is extremely sensitive to subtle local distortions and charge polarization, because the EFG is determined primarily by the electrons involved in the bonding with the nearest neighbors. For half-integer nuclear spin the lowest transition frequency is given by $\omega_0 = 6\omega_{\mathrm{Q}}$.

If the EFGs at the sites of the different probe atoms vary around a mean value (or about 0 in a cubic lattice), e.g., as due to a distribution of point defects on the lattice, which are not necessarily in the neighborhood nor correlated with the probe atom that originates a distribution of slightly different EFGs. In a γ-γ angular correlation time spectrum, this effect leads to a damping of the G(t) oscillations in time, which, for the case of a Lorentzian EFG distribution, modifies the perturbation function as shown below:

$$\mathrm{G_{22}\,(t)} = \mathrm{s_{20}} + \sum_{\mathrm{n=1}}^{3} \mathrm{s_{2n}cos\,(n\omega_n t)e^{-n\sigma t}} \tag{5}$$

with $\sigma = \Delta\omega/2\pi \propto \Delta \mathrm{V_{zz}}$

From the experimental point of view, gamma scintillation detectors and nuclear electronic modules are used to select and store histogram spectra of γ_1-γ_2 coincidences, $\mathrm{N_j}(\theta,\mathrm{t})$, distributed as a function of time between detection of γ_1 (start) and γ_2(stop). These are recorded for each pair of detectors, j = 1-30 (6 detectors) or j= 1-12 (4 detectors), at detector angles of $\theta = 90°$ and $\theta = 180°$. After subtraction of a constant background due to accidental coincidences originating from gamma rays emitted from different nuclei the multiple spectra, $\mathrm{W_j}(\theta,\mathrm{t})$ are combined to correct for different efficiencies and small sample misalignments and emphasize the perturbation time spectra, the PAC observable function, R(t):

$$R\,(t) = 2.\left(\frac{W\left(180^o,t\right) - W\left(90^o,t\right)}{W\left(180^o,t\right) + 2W\left(90^o,t\right)}\right) \sim A_{22}G_{22}\,(t) \tag{6}$$

3 PAC isotopes

The cyclotron-produced **^{111}In(^{111}Cd)** is a common PAC probe that is introduced into the samples via diffusion, implantation or chemical processes. **^{111}In** decays with a half-life of 2.8 days by electron capture to an excited state of ^{111}Cd. The ^{111m}Cd decays to its ground state by emitting two successive γ-quanta via an intermediate state with $Q = +0.683(20)$ b [12] and $\mu = -0.7656(25)\mu_N$ [10] which is used for PAC measurements. Due to the relatively long half-life value of the intermediate state of 85 ns, studies of *after effects* (long standing electronic excitations due to uncomplete atomic shell filling after nuclear transmutation) [13, 14], magnetic or/and electric hyperfine interactions on a time scale of around 400 ns are possible. In this work, the ^{111}In has been implanted at ISOLDE during the ^{111m}Cd implantation.

^{111m}Cd(^{111}Cd) is also a conventional PAC probe and can be obtained online at ISOLDE by proton bombardment of a molten Sn target. Its short half-life of 48.5 minutes generally limits one PAC measurement to one sample preparation (annealing + one measuring temperature), thus requiring many samples and repeatedly reproducible sample preparations. The great advantage of using this probe is that there is no element transmutation involved in its decay. Particularly, combined studies of ^{111m}Cd/Cd incorporation using $\gamma - \gamma$ PAC can help to disentangle static or dynamic electronic phenomena through the comparison with ^{111}In/Cd measurements.

4 Experimental

TiO_2 (100) single crystals with 99.6 % purity were obtained commercially by Goodfellow. PAC experiments were performed following 30 keV implantation of low dose $<2.10^{11}$ at/cm^2, with $\sim 5.10^{10}$ atoms of ^{111m}Cd per sample. On some samples, $\sim 2.10^{10}$ atoms of ^{111}In were co-implanted along with ^{111m}Cd due to overheating of the transfer line of the ISOLDE target. Subsequent annealing at 873 K, 10 min, under vacuum of 10^{-5} mbar was performed for all samples. These measurements were carried out at different temperatures up to 693 K. The Q value we used is reported on the work from Haas et al. [12]

5 Results

Since the same intermediate, $(5/2)^+$, 245 keV probing state on ^{111}Cd is obtained upon decay of ^{111}In and ^{111m}Cd, the observable EFGs there obtained are easily compared, particularly for the ^{111}In/^{111m}Cd co-implanted sample with the same implantation and annealing treatment history. The fact that ^{111}In has a much longer half-life than ^{111m}Cd and the use of La(Ce)Br_3 detectors, which are able to separate the first gamma ray of 150 keV upon decay of ^{111m}Cd from the first gamma ray of 170 keV upon decay of ^{111}In, allow to perform both experiments on the same sample. Firstly, the PAC experiments are performed on the decay of ^{111m}Cd/Cd followed by the measurement on ^{111}In/Cd.

Figure 1a and b show $\gamma - \gamma$ PAC R(t) data obtained upon decay of ^{111m}Cd/Cd, measured at room temperature and at 465 K. Figure 1c shows the data obtained upon decay of ^{111}In/Cd measured on the same sample as of Fig. 1b, but at room temperature. In spite of being observed a reduction of R(t) amplitude on ^{111}In/Cd data, with about 30 % missing observable amplitude, only the characteristic EFG for Cd occupying Ti sites on TiO_2 is observed, that is characterized, by $\omega_{01} = 99.01(16)$ Mrad/s and a small $\eta_1 \sim 0.175(12)$.

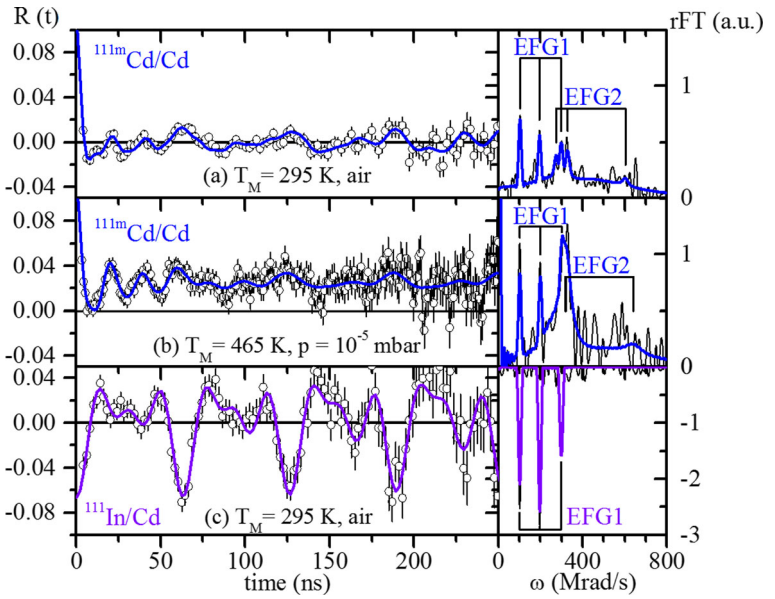

Fig. 1 Experimental $\gamma - \gamma$ R(t) perturbation functions obtained for ^{111m}Cd/Cd at 295 K (**a**) and at 465 K (b) and ^{111}In/Cd (c) PAC probes on TiO_2. Additionally, their real part of the R(t) Fourier transform. Measurement temperature and pressure are quoted on each spectrum. Spectra (b) and (c) belong to the sample that were implanted with ^{111m}Cd and ^{111}In simultaneously

The missing fraction f_d in spectra displayed in Fig. 1c could either be explained by a strong damping due to a strong distribution of remaining defects or by the so called after effect, that could not be further investigated on the present set of experiments.

Noticeably, the behavior of the ^{111}In/Cd data is clearly different from the measurements performed with ^{111m}Cd/Cd, where a big fraction of nuclei, f_d = 48(5) and 78(6) % on different samples, are characterized by a very strong EFG distribution leading to a significant initial damping on the R(t) spectra clearly visible on Fig. 1a and b. The ^{111m}Cd/Cd data further shows a second EFG_2 distribution, characterized by $\omega_{02} = 180(1)$ Mrad/s and a big η_2 ˜0.79(1) at 295K or η_2 ˜0.99(3) at 465 K, of which the fraction varies with the sample and measurement temperature. Table 1 summarizes the resulting hyperfine fitting parameters.

Table 1 Hyperfine fitting parameters of PAC experiments performed in TiO_2 single crystals

Spectrum		$T_M(K)$	*EFG*	w_0*(Mrad/s)*	η	σ (Mrad/s)	Fraction (%)
implanted^{111m}Cd/Cd	a	295	1	98.7(4)	0.21(2)	1.2(1)	11(1)
			2	180(1)	0.79(1)	2.9(1)	12(1)
			d	*235(8)*	*0*	*117(10)*	*78(6)*
implanted^{111m}Cd/Cd +^{111}In/Cd	b	465	1	100.0(7)	0.15(2)	0.0(1)	12(2)
			2	182(2)	0.99(3)	15(2)	42(3)
			d	*257(14)*	*0*	*68(16)*	*48(5)*
	c	295	1	99.01(16)	0.175(12)	0(1)	70
			d	–	–	–	*30*

6 Discussion

Firstly, the unique EFG pattern that it is measured with ^{111}In/Cd, leads to believe that the Cd environment after In decay is rich on charge carriers and mobile electrons, allowing a fast recombination of the electronic shells after electron capture, thus hindering a significant after effect, that could not be further investigated on the present work. But the results clearly show that the hyperfine interactions observed at ^{111}Cd from ^{111}In or ^{111m}Cd decay are quite different. ^{111}In/Cd shows a single site fraction with quadrupole frequency and asymmetry parameter values similar to that observed for the same probe nuclei in bulk TiO_2 oxides. Results for ^{111m}Cd/Cd show two site fractions, one with hyperfine parameters similar to those observed for ^{111}In/Cd and another one with quadrupole frequency and asymmetry parameters with higher values as was already observed in thin films [7]. These results indicate that, although the probe nuclei are the same, ^{111}Cd at the 245 keV level, the parent nuclei have influenced the hyperfine parameters. Ti atoms have valence +4 whereas In and Cd atoms have valences +3 and +2, respectively, suggesting that a necessary charge compensation when these atoms replace Ti at cationic sites is necessary. In fact, first principles calculations reported in the literature [15] show that the experimental values for the principal component of the EFG and the asymmetry parameter roughly reproduce the experimental values for EFG1, $V_{zz} = 6.4(4) \times 10^{21}$ V/m^2 and eta = 0.18(1), from the present work, when a charge compensation of two electrons is considered ($V_{zz} = 4.6 \times 10^{21}$ V/m^2 and $\eta = 0.26$). Interestingly the parameters observed for the second site fraction measured with ^{111m}Cd/Cd, $V_{zz} = 11.6(9) \times 10^{21}$ V/m^2 and $\eta = 0.81(1)$ are also similar to those found from calculations without charge compensation, $V_{zz} = -7.16 \times 10^{21}$ V/m^2 and $\eta = 0.91$ [15]. For EFG2 there is a significant temperature dependence on V_{zz}, η and broadening, between room temperature and 465K. This fact further points for an important temperature dependent "defect" or "electronic defect" local configuration in the Cd surroundings. These data further suggests that the charge compensation for Cd doping from ^{111}In implantation is easier, and probably faster, than that for Cd doping from ^{111m}Cd implantation, for which part of the Cd atoms are compensated and part are not. Moreover, the uncompensated fraction is probably due to oxygen vacancies in the neighborhood of Cd impurities which are induced by the valence difference as previously reported for Cd impurities in In_2O_3 oxide [16]. A particularly interesting case to study the influence of the valence state on the dopant site and interaction with defects, upon ion doping implantation on TiO_2 rutile, would be to use the complementary ^{111}Ag/Cd PAC probe with valence state +1. Das et al. [17] have performed ^{111}Ag/Cd studies and found quite different EFGs than the ones presently reported. However, their sample preparation methodology, with ^{111}Ag being introduced during sample's synthesis hinder a comparative discussion due the unknowns regarding site occupancy or interactions with similar point defects to the ones produced upon ion implantation. Such studies are definitely possible and envisaged to be performed at ISOLDE in the near future.

The *missing / attenuated* fractions f_d could still be interpreted as due to the remains of unrecovered distributions of defects, which do not establish well defined configurations with the Cd probing atoms. Electronic dynamic instabilities such as the ones assigned to *after effects* cannot be present in the experiments performed with ^{111m}Cd/Cd γ-γ PAC, where a very strong unidentified loss of anisotropy is also observed that can only be attributed to a (static) distribution of defects and, furthermore, a second EFG_2 distribution is additionally identified. We further point out that upon decay of ^{111}In, the ^{111}Cd atom gets a small recoil energy of about 1 eV that might still be enough to displace some of the Cd atoms leaving it free to interact with remaining lattice defects and contribute to the missing anisotropy.

Still, we believe that another explanation is more plausible. With the present 30 keV ion beam energy the ions roughly reach 15 nm below the surface, probably leading to a fraction of ^{111}In and ^{111m}Cd atoms to be placed on zones with intrinsic defects, which cannot be annealed at all, yielding strongly damped EFGs distributions. Indium seems not to attract oxygen vacancies at the applied partial pressures. Thus, the spectrum is clearly that of a substitutional atom. Cd can attract the vacancies according to partial pressure. The *missing / attenuated* fractions are likely due to multiple attracted vacancies (or charging / discharging vacancies) that alter the environment.

7 Conclusions

PAC experiments performed on ^{111}In/Cd and ^{111m}Cd/Cd PAC probes from the same implantation show the presence of a main clear electric quadrupole interaction, described by EFG_1 which was assigned to Cd atoms placed on Ti sites at the Rutile phase of TiO_2. However, implanted In and Cd behave different under the same implantation and annealing procedures. While ^{111}In/Cd seems to be free of point defects after annealing, the implanted ^{111m}Cd/Cd acts as highly stable "trap" for defects. A second highly asymmetric EFG_2 has been measured when implanting ^{111m}Cd. Its interpretation requires further studies, where Density Functional Theory (DFT) will be used to simulate the interaction of Cd with, e.g., oxygen vacancies on the Rutile lattice. Additionally, in all cases, a big fraction of atoms, f_3, shows no identifiable fields but strong EFG distributions responsible for the missing anisotropy in all experiments. We hint this to be due to the shallow implantation depth of the In and Cd atoms remaining in a zone of intrinsic defects near surface. Finally, there is no evidence for the existence of after effects observable during ^{111}In PAC experiments. Surely the concentration of electron carriers, and electron mobility, must be high enough allowing for fast recombination, below ns, of the atomic shells involved in the electron capture nuclear transmutation or electron conversion processes for the ^{111}In/Cd and ^{111m}Cd/Cd, respectively. These studies demonstrate the interest and potentialities of the ISOLDE laboratory in producing exotic radioactive isotopes, which are suitable for the use of combined hyperfine PAC techniques there available. Further studies are envisaged on different doped materials, single crystals, thin films and nanoparticles.

Acknowledgments The research leading to these results has received funding from the European Union's Horizon 2020 research and innovation programme under grant agreement 654002, from Federal Ministry of Education and Research (BMBF) through grants 05K13TSA and 05K16PGA, from the FCT project CERN-FIS-NUC-0004-2015. We thank very much A. T. Martín-Luengo from the Institut für Halbleiter-und-Festkörperphysik, Johannes Kepler Universität for helping to carry out the measurements. A. M. Lima Lopes together with her team from Portugal and the ISOLDE in-house group are thankfully acknowledged for great discussions and technical assistance during the shared beam time.

References

1. Chen, H., Wei, Z., Yan, K., Bai, Y., Yang, S.: Unveiling two electron-transport modes in oxygen-deficient TiO2 nanowires and their influence on photoelectrochemical operation. J. Phys. Chem. Lett. **5**, 2890–2896 (2014)
2. Choi, W., Termin, A., Hoffmann, M.R.: The role of metal ion dopants in quantum-sized TiO_2: Correlation between photoreactivity and charge carrier recombination dynamics. J. Phys. Chem. **98**, 13669–13679 (1994)

3. Liu, B., Chen, H.M., Liu, C., Andrews, S.C., Hahn, C., Yang, P.: Large-scale synthesis of transition-metal-doped TiO_2 nanowires with controllable overpotential. J. Am. Chem. Soc. **135**, 9995–9998 (2013)
4. Li, Y., Guo, Y., Li, Y., Zhou, X.: Fabrication of Cd-Doped TiO_2 nanorod arrays and photovoltaic property in perovskite solar cell. Elec. Acta **200**, 29–36 (2016)
5. Zaleska, A.: Doped-TiO_2: a review. Recent Patents on Engineering **2**, 157–164 (2008)
6. Adams, J.M., Catchen, G.L.: Anomalous crystal chemistries of the $^{111\rightarrow111}$Cd and $^{181\rightarrow181}$Ta probes in rutile TiO_2 studied using perturbed-angular-correlation spectroscopy. Phys. Rev. B **50**, 1264–1267 (1994)
7. Schell, J.: Investigation of hyperfine parameters in pure and 3d transition metal doped SnO_2 and TiO_2 by means of perturbed gamma-gamma angular correlation spectroscopy. CERN-THESIS-2015-229. São Paulo University, Brazil (2015)
8. Darriba, G.N., Errico, L.A., Eversheim, P.D., Fabricius, G., Renteria, M.: First-principles and time differential $y - y$ perturbed-angular-correlation spectroscopy study of structural and electronic properties of Ta-doped TiO_2 semiconductor. Phys. Rev. B **79**, 115213/1–115213/12 (2009)
9. Banerjee, D., Das, S.K., Thakare, S.V., Nabhiraj, P.Y., Menon, R., Bhandari, R.K., Krishnan, K.: Study of surface-bulk mass transport and phase transformation in nano-TiO_2 using hyperfine interaction technique. J. Phys. Chem. Sol. **71**, 983–987 (2010)
10. Schatz, G., Weidinger, A.: Nuclear condensed matter physics: nuclear methods and applications. Wiley, Chichester (1996)
11. Abragam, A., Pound, R.V.: Influence of electric and magnetic fields on angular correlations. Phys. Rev. **92**, 943–962 (1953)
12. Haas, H., Barbosa, M.B., Correia, J.G.: The quadrupole moments of Cd and Zn isotopes - an apology. Hyp. Int. Accepted for publication (2016)
13. Lupascu, D., Habenicht, S., Lieb, K.P., Neubauer, M., Uhrmacher, M., Wenzel, T.: Relaxation of electronic defects in pure and doped La_2O_3 observed by perturbed angular correlations. Phys. Rev. B **54**, 871–883. 1996
14. Lupascu, D., Neubauer, M., Wenzel, T., Uhrmacher, M., Lieb, K.P.: Perturbed angular correlations in metal oxides with radioactive tracer beams. Nucl. Instrum. Meth. Phys. Res. B **113**, 507–512 (1996)
15. Errico, L.A., Fabricius, G., Renterıa, M., de La Presa, P., Forker, M.: Anisotropic Relaxations Introduced by Cd impurities in rutile TiO_2: first-principles calculations and experimental support. Phys. Rev. Lett. **89**, 055503/1–055503/4 (2002)
16. Sena, C., Costa, M.S., Muñoz, E.L., Cabrera-Pasca, G.A., Pereira, L.F.D., Mestnik-Filho, J., Carbonari, A.W., Coaquira, J.A.H.: Charge distribution and hyperfine interactions in the vicinity of impurity sites in In_2O_3 doped with Fe, Co, and Ni. J. Magn. Magn. Mater. **387**, 165–178 (2015)
17. Das, S.K., Thakare, S.V., Butz, T.: The nuclear quadrupole interaction at ^{111}Cd and ^{181}Ta sites in anatase and rutile TiO_2: A TDPAC study. J. Phys. Chem. Sol. **70**, 778–781 (2009)